



Cite this: *Dalton Trans.*, 2024, **53**, 11445

Facile synthesis and bonding of 4-ferrocenyl-1,2,4-triazol-5-ylidene complexes†

Michal Franc, Jiří Schulz and Petr Štěpnička *

Ferrocene-substituted carbenes have emerged as attractive, redox-active ligands. However, among the compounds studied to date, ferrocenylated 1,2,4-triazol-5-ylidenes, which are closely related to the archetypal imidazol-2-ylidenes, are still unknown. Here, we demonstrate that the triazolium salt $[\text{CHN}(\text{Me})\text{NCHN}(\text{Fc})]\text{I}$ (**2**; Fc = ferrocenyl), obtained by alkylation of 4-ferrocenyl-4*H*-1,2,4-triazole (**1**) with MeI, reacts selectively with metal alkoxide/hydroxide precursors $[(\text{cod})\text{Rh}(\text{OMe})_2]$ and $[(\text{IPr})\text{Au}(\text{OH})]$ (cod = cycloocta-1,5-diene, IPr = 1,3-bis(2,6-diisopropylphenyl)imidazol-2-ylidene) to produce the ferrocene-substituted 1,2,4-triazol-5-ylidene complexes $[(\text{cod})\text{Rh}\{(\text{CN}(\text{Me})\text{NCHN}(\text{Fc}))\}]$ and $[(\text{IPr})\text{Au}(\text{CN}(\text{Me})\text{NCHN}(\text{Fc}))]$ in good yields. The complexes were characterised by NMR and IR spectroscopy, mass spectrometry, cyclic voltammetry, and single-crystal X-ray diffraction analysis. Density function theory (DFT) calculations were used to rationalise the electrochemical behaviour of the carbene complexes and to elucidate the bonding situation in these compounds. An analysis using intrinsic bond orbitals (IBOs) revealed that the 1,2,4-triazol-5-ylidene ligand exerted a strong *trans* influence and showed a synergistic stabilisation by the negative inductive and positive π -donor effects of the nitrogen atoms adjacent to the carbene carbon atom; these effects were enhanced by conjugation with the $\text{CH}=\text{N}$ bond at the exterior, similar to that in imidazol-2-ylidenes.

Received 15th May 2024,
Accepted 17th June 2024
DOI: 10.1039/d4dt01433b
rsc.li/dalton

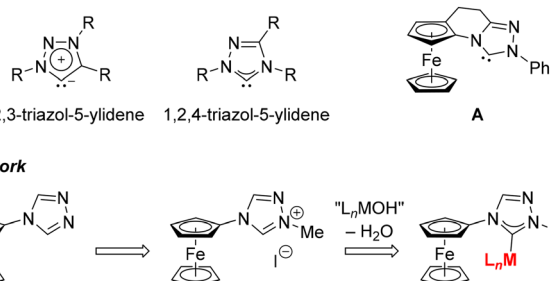
Introduction

Pioneering experiments by Wanzlick¹ and Öfele² in the 1960s and subsequent isolation of the first³ N-heterocyclic carbene (NHC) three decades later⁴ opened a new, exciting area of chemistry. The discovered NHCs were rapidly recognised as attractive ligands for transition metals and metal-mediated reactions and as organocatalysts, which further accelerated the research focused on these compounds.⁵ Soon, the family of NHCs, which were originally derived from imidazoles, was expanded to include compounds based on other heterocyclic scaffolds, such as pyrrolidine, thiazole, and triazoles.⁵

In this regard, carbenes resulting from readily accessible⁶ 1,2,3-triazoles (*i.e.*, 1,2,3-triazol-5-ylidenes), reported first in 2008,⁷ have a distinct position as examples of mesoionic carbenes, whose structures cannot be shown without adding charges to some of the ring atoms (Scheme 1). In contrast, iso-

meric compounds derived from 1,2,4-triazoles (*i.e.*, 1,2,4-triazol-5-ylidenes), which can be regarded as imidazol-2-ylidene analogues with an additional nitrogen atom inserted in the ring, are less explored^{8,9} even though they are equally structurally versatile and widely applicable. Thus far, 1,2,4-triazolylidenes have been used as auxiliary ligands in the design of transition metal catalysts,¹⁰ new luminescent materials¹¹ and biologically active compounds,¹² and further utilised as organocatalysts.¹³

Despite their wide applications, 1,2,4-triazol-5-ylidenes have not yet established themselves among the ferrocene car-



Scheme 1 (top) General structures of 1,2,3- and 1,2,4-triazol-5-ylidenes and the ferrocene-based 1,2,4-triazol-5-ylidene **A**, and (bottom) the aim of this work.

Department of Inorganic Chemistry, Faculty of Science, Charles University, Hlavova 2030, 128 40 Prague, Czech Republic. E-mail: stepnic@natur.cuni.cz

† Electronic supplementary information (ESI) available: Synthesis of **1** and **2**, details on structure determination and additional structure diagrams, computational details and further results from DFT calculations, copies of the NMR spectra (PDF file), and Cartesian coordinates of the DFT-optimised structures (XYZ file). CCDC 2345618 and 2345619. For ESI and crystallographic data in CIF or other electronic format see DOI: <https://doi.org/10.1039/d4dt01433b>



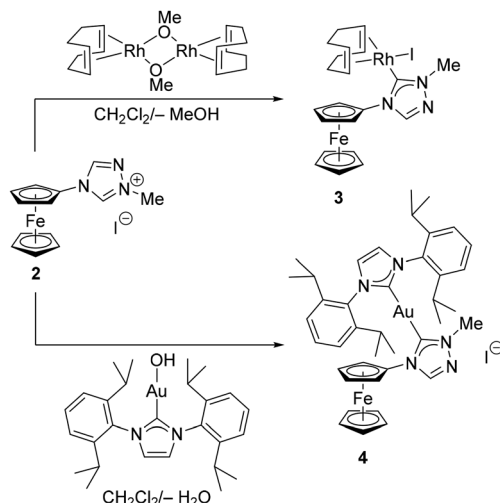
benes,¹⁴ unlike their 1,2,3-isomers, which have been studied as redox-active and redox-switchable ligands.¹⁵ To the best of our knowledge, the sole exception is the planar chiral carbene **A** (Scheme 1), which was trapped and structurally authenticated as a CuCl complex.^{16,17} Based on this, we decided to synthesise and study the 1,2,4-triazol-5-ylidene complexes derived from 4-ferrocenyl-4*H*-1,2,4-triazole (**1**),¹⁸ which bears the ferrocenyl substituent directly at the triazole ring. The synthesis was accomplished by using simple reactions of the corresponding triazolium salt with suitable metal hydroxide and alkoxide complexes¹⁹ that act as both the base and the metal source.

Results and discussion

The parent azole, 4-ferrocenyl-4*H*-1,2,4-triazole (**1**),¹⁸ was prepared by acid-catalysed condensation of aminoferrocene²⁰ with *N,N'*-bis(dimethylaminomethylene)hydrazine²¹ in refluxing toluene (Scheme 2) and isolated in a 70% yield after chromatography (see the ES[†]).²² Subsequent alkylation with methyl iodide produced triazolium salt **2**²³ (88% yield). Attempts to obtain a doubly methylated derivative²⁴ (as an entry to biscarbene complexes²⁵) by reacting **1** with an excess of MeI or [Me₃O][BF₄] or, alternatively, by reacting **2** with [Me₃O][BF₄] were unsuccessful.²⁶

The ¹H and ¹³C{¹H} NMR spectra of **1** showed the resonances due to the ferrocenyl substituent, with the signal of C^{ipso}-N characteristically shifted to a low field (δ_{C} 90.5; cf. δ_{C} 105.6 for aminoferrocene²⁷). The signals of the triazole ring (CH=N) were detected at δ_{H} 8.36 and δ_{C} 143.0 (in CDCl₃). Upon alkylation, the ¹H and ¹³C{¹H} NMR signals of the ferrocene CH groups shifted to a lower field, while the C^{ipso}-N signal moved slightly upfield (δ_{C} 89.3 in CD₂Cl₂/CD₃OD). Methylation also differentiated the triazole CH groups, particularly in the ¹H NMR spectrum (δ_{H} 8.50, 11.6; δ_{C} \approx 142.3 for both carbons); the signal of the methyl substituent was observed at δ_{H} 4.36 and δ_{C} 42.0.

Compound **2** cleanly reacted with [Rh(μ -OMe)(cod)]₂ (cod = 1,5-cycloocta-1,5-diene) in dry dichloromethane to produce carbene complex **3** (Scheme 3),²⁸ which was obtained in 73% yield after column chromatography. Compound **3** was stable under ambient conditions and dissolved well in common organic solvents, which made its crystallisation difficult. Crystals suitable for structure determination were eventually grown by diffusion of water vapour into a solution of the complex in acetone, which further illustrated the high chemi-



Scheme 3 Synthesis of carbene complexes **3** and **4**.

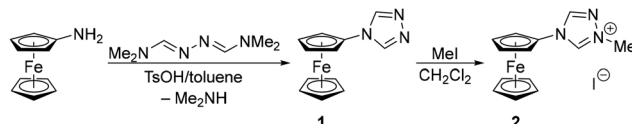
cal stability of this compound. In contrast, the complex decomposed when treated with MeI or [Me₃O][BF₄].

Similarly, the triazolium salt underwent a smooth reaction with the Au(I) hydroxide [(IPr)Au(OH)]²⁹ (IPr = 1,3-bis(2,6-diisopropylphenyl)imidazol-2-ylidene- κ C²), generating bis-carbene complex **4** (Scheme 3),³⁰ which was isolated by flash chromatography in a 90% yield. Even in this case, further methylation with MeI or Meerwein salt was not successful.

The formation of carbene complexes was indicated by their distinct NMR features. In particular, the ¹³C{¹H} NMR spectrum of **3** displayed a low-field signal attributable to the carbene carbon (δ_{C} 185.9), split into a doublet by ¹⁰³Rh ($^1J_{\text{C}-\text{Rh}} = 49$ Hz). Because of hindered molecular mobility, the CH groups in the ferrocene C₅H₄ ring were diastereotopic and produced four separate signals in the ¹H and ¹³C{¹H} NMR spectra, and similar features were observed for the CH and CH₂ signals of the diene ligand. The ¹³C NMR signals of the η^2 -coordinated double bonds were observed at δ_{C} 71.9/72.5 (d, $^1J_{\text{C}-\text{Rh}} = 14$ Hz) and 96.3/96.9 (d, $^1J_{\text{C}-\text{Rh}} = 7$ Hz), being markedly distinguished by ligands in the *trans* positions.

For **4**, two carbene ¹³C NMR signals were observed at δ_{C} 183.5 (triazolylidene) and 185.5 (IPr). Unlike **3**, however, the signals of the ferrocene unit in **4** were degenerate; specifically, only two signals were found for the CH groups at the C₅H₄ ring, and even the resonances of the isopropyl substituents at the IPr ligand were undifferentiated despite the overall steric bulk. The electrospray ionisation (ESI) mass spectra showed ions due to [M – I]⁺ resulting from ligand loss (**3**) and simple dissociation (**4**).

Structure determination of **3** (Fig. 1) revealed square planar coordination around the Rh(I) centre with η^2 -coordinated double bonds oriented nearly perpendicular to the plane defined by the rhodium and the remaining donor atoms {Rh1, I1, C11} (angles 82.3(1) $^\circ$ and 81.0(1) $^\circ$ for the C21=C22 and C25=C26 bonds, respectively). The individual Rh-C distances (Rh1-C21 2.118(2), Rh1-C22 2.124(2), Rh1-C25 2.209(2), and



Scheme 2 Preparation and alkylation of 4-ferrocenyl-4*H*-1,2,4-triazole (**1**) (TsOH = 4-toluenesulfonic acid).



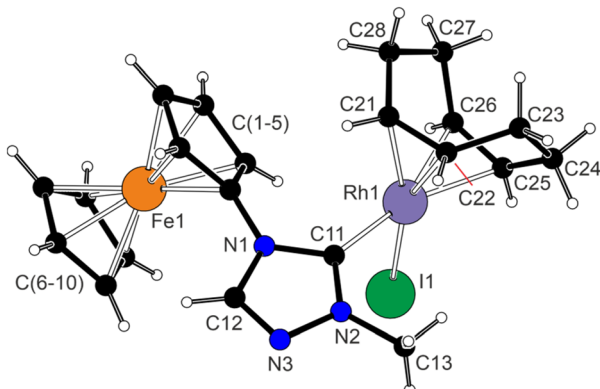


Fig. 1 Molecular structure of **3**.

Rh1–C26 2.220(2) Å varied, depending on the *trans* influence of the remaining ligands (carbene > I),^{31,32} in agreement with the NMR data; the C=C bond lengths were inversely affected (C21–C22 1.410(3) Å, C25–C26 1.373(3) Å).

The Rh1–C11 distance in **3** (2.016(2) Å) did not significantly differ from those in the analogous complexes featuring ring-fused triazolylidenes³³ and triazolium-ylidene ligands,³⁴ while the Rh1–I1 bond (2.6849(4) Å) had a similar length as that in [Rhi(cod)L] (L = 1,3-dimethylimidazolin-2-ylidene).^{28b} The ferrocene unit in **3** showed similar Fe–C distances (2.032(2)–2.052(2) Å) and only minor tilting³⁵ of the cyclopentadienyl rings (4.0(1)°).

The structure of **4**·CHCl₃ (Fig. 2) comprised symmetrically and linearly coordinated Au(I) ion (Au1–C11 2.020(4), Au1–C21 2.016(4) Å; C11–Au1–C21 178.5(2)°); the Au–C distances were unexceptional considering those reported for the symmetrical complexes [Au(IPr)₂][BF₄]³⁶ and [AuL₂][AuI₂] (L = 1,4-dimethyl-1,2,4-triazol-5-ylidene).³⁷ The carbene moieties in **4** were mutually twisted by 20.4(3)°, and the triazolylidene ring was rotated by 21.6(3)° from the plane of the cyclopentadienyl ring C(1–5). The ferrocene unit had its usual geometry with parallel cyclopentadienyl rings (Fe–C 2.022(4)–2.054(5) Å, tilt: 0.8(3)°).

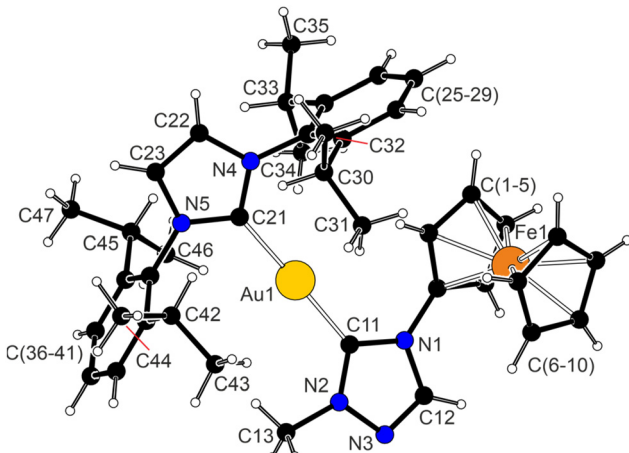


Fig. 2 View of the complex cation in the structure of **4**·CHCl₃.

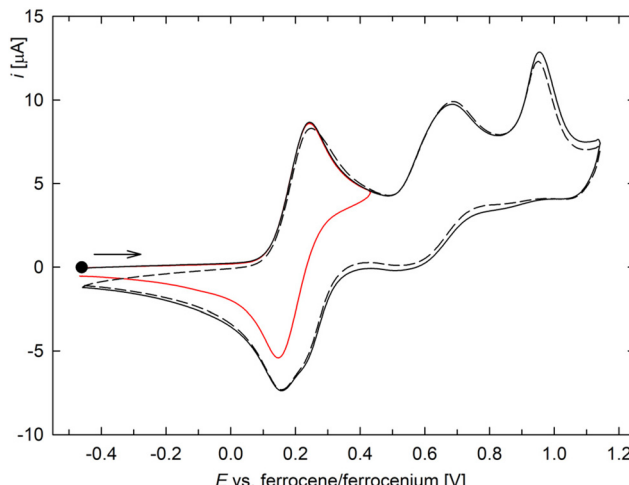


Fig. 3 Cyclic voltammograms of **3** (glassy carbon disc electrode, dichloromethane, 0.1 M Bu₄N[PF₆], scan rate: 100 mV s⁻¹). The scan direction is indicated with an arrow, and the voltammograms recorded over different potential ranges are distinguished by colour; the second scan is shown as a dashed line.

While the structure of **3** was essentially molecular, the cooperative, soft hydrogen bonds between the polarised CH groups at the carbene ligands and the halogen atoms (the iodide anion and chlorine from the solvent molecule) were detected in the crystal assembly of ionic **4**·CHCl₃ (see the ESI, Fig. S3†).

The complexes were studied by cyclic voltammetry at a glassy carbon electrode in dichloromethane containing [Bu₄N][PF₆] (0.1 M) (data for triazole **1** are presented in the ESI†). The redox behaviour of Rh(I) complex **3** was relatively complicated (Fig. 3): the compound underwent one-electron oxidation at 0.19 V *vs.* the ferrocene/ferrocenium reference,³⁸

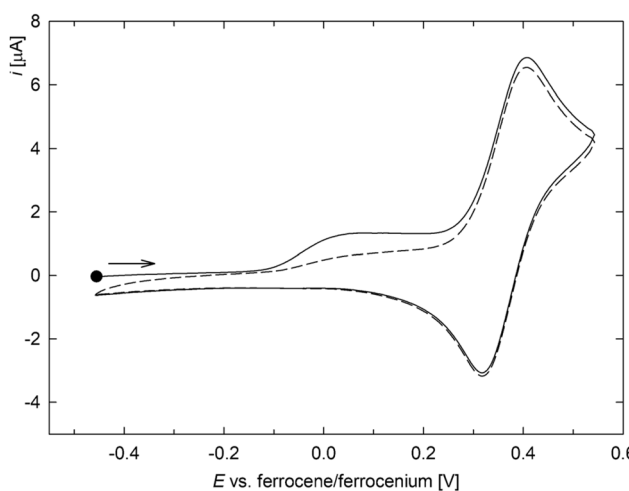


Fig. 4 Cyclic voltammogram of **4** (glassy carbon disc electrode, dichloromethane, 0.1 M Bu₄N[PF₆], scan rate: 100 mV s⁻¹). The scan direction is indicated with an arrow, and the second scan is shown as a dashed line.

which was followed by two irreversible redox steps at approximately 0.68 and 0.95 V (the anodic peak potentials at a scan range of 100 mV s⁻¹ are given).³⁹ The peak currents of the two irreversible oxidations were lower than that of the first reversible oxidation step, and the shape of the last oxidation indicated the possible involvement of adsorption phenomena. After traversing the second oxidative step, the cathodic branch of the first wave gained a “shoulder” as a result of convolution with a minor reductive wave due to an electrochemically generated species.

In contrast, complex **4** displayed single reversible oxidation at 0.32 V, which was preceded by a relatively weaker, broad peak, likely due to adsorbed species (Fig. 4). The oxidation occurred at a more positive potential than that of **3**, in line with the cationic nature of complex **4** and with the absence of the purely donor ligands in the structure (the carbenes are π -acceptors), both making electron removal more difficult.

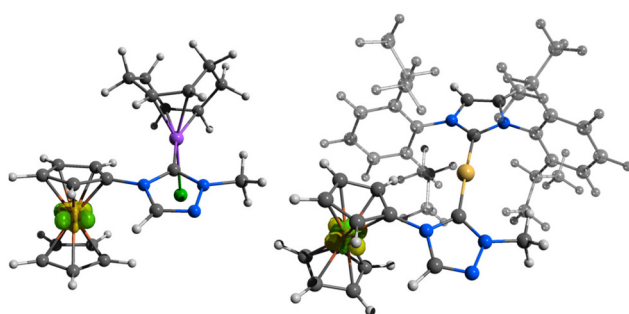


Fig. 5 Electron difference maps for $\rho(3) - \rho(3^+)$ (left), and $\rho(4) - \rho(4^+)$ (right; only the cation is shown for clarity) mapped at the geometry of the native species **3** and **4** (isosurfaces at ± 0.02 a.u.).

An analysis of the frontier molecular orbitals (FMOs) using the natural atomic orbital (NAO) approach⁴⁰ revealed that both HOMO and LUMO of complex **3** were localised mainly at the Rh(cod)I fragment, while for **4**, the HOMO was confined to the ferrocene unit, and the LUMO was evenly distributed between the two Au-bound carbene ligands (for details, see ESI†). However, to rationalise the electrochemical behaviour, we investigated electron density changes associated with electron removal.⁴¹ Indeed, the calculated electron density change between the parent species and its oxidized form with the same geometry, $\rho(3) - \rho(3^+)$ and $\rho(4) - \rho(4^+)$, indicated that the initial oxidation indeed occurs at the ferrocene moiety (Fig. 5).

The bonding of the carbene complexes was investigated using intrinsic bond orbitals (IBOs).⁴² For complex **3**, the bonding situation could be effectively described by the traditional Dewar–Chatt–Duncanson model:⁴³ the diene ligand transfers four electrons from the bonding π orbitals of the two C=C bonds to a metal-centred vacant orbital (Fig. 6), while the metal donates electrons back to the antibonding $\pi^*(C=C)$ orbitals. However, a closer inspection of the IBOs describing these interactions showed that the coordination of the diene to the rhodium was asymmetrical, with the asymmetry reflecting the different *trans* influence of the other ligands:⁴⁴ the coordination of the double bond in the *trans* position to the carbene ligand [0.84(C25):0.88(C26)/0.24(Rh)] was weakened compared to that of the double bond located *trans* to the iodide ligand [0.77(C21):0.84(C22)/0.36(Rh)]. A lower π donation diminished Rh–C=C π -back donation [1.73(Rh)/0.12(C25):0.11(C26)]. Both effects were reflected in the different Rh–C bond lengths, as determined experimentally (*vide supra*) and calculated (Table 1), and in the different bond orders of the non-equivalent double bonds. The calculated

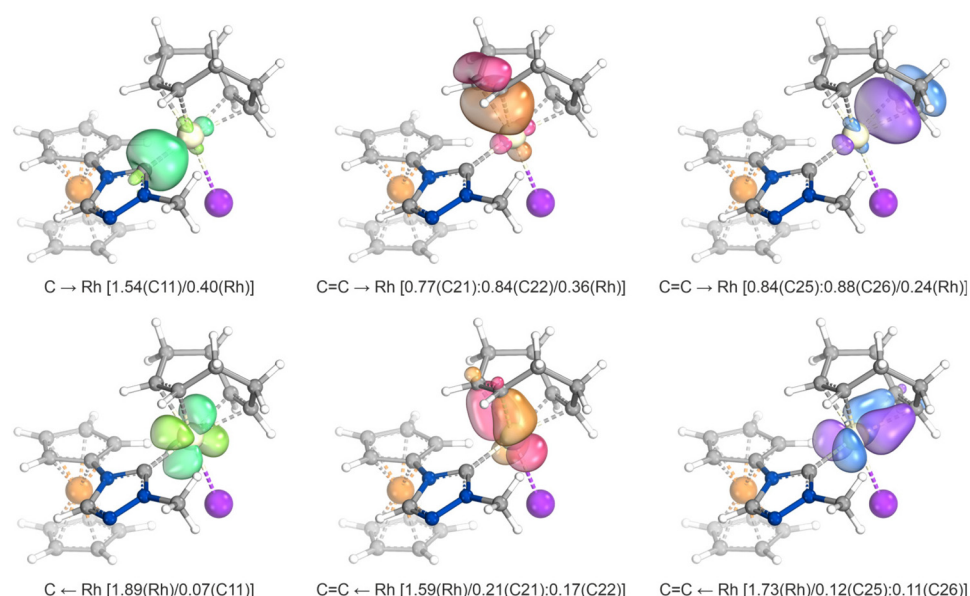


Fig. 6 Selected intrinsic bond orbitals (IBOs) of **3**. The values in parentheses indicate the fraction of the bonding electrons assigned to the individual atoms. Atom labelling follows that in the crystal structure (see Fig. 1). The IBO corresponding to the standard I→Rh dative bond with the following parameters is not shown [1.64(I)/0.29(Rh)].



Mayer bond order of the C=C bond *trans* to the carbene ligand was greater (MBO 1.42), reflecting a lower back-donation to the antibonding $\pi^*(\text{C}=\text{C})$ orbitals, while the increased Rh \rightarrow C=C interaction [1.59(Rh)/0.21(C21):0.17(C22)] weakened the C=C bond in the *trans* position with respect to the iodide ligand (MBO 1.23).

The IBOs describing the Rh–carbene [1.54(C)/0.40(Rh)] and Rh–I bonds [1.64(C)/0.29(Rh)] showed values typical of L-type,⁴⁵ dative σ interactions. For the carbene, the σ interaction was supported by Rh \rightarrow C^{triaz} π -back bonding [1.89(Rh)/0.07(C)], albeit less than for the cod ligand.

IBO analysis of complex **4** focused mainly on the comparison between the two carbene ligands. Both carbenes coordinated as L-type ligands, with the σ -bonding component dominating over π -back bonding (Fig. 7).⁴⁶ The donor properties of both ligands were rather similar, although the IPr ligand appeared to be a better σ donor (based on the comparison of charge distribution in the respective IBOs: [1.54(C^{IPr})/0.40(Au)] *vs.* [1.56(C^{triaz})/0.38(Au)]), whereas the triazolylidene ligand behaved as a better acceptor ([1.91(Au)/0.03(C^{IPr})/0.04(C^{triaz})])�.

Further analysis, focused on the bonding within the carbene ligands (see the ESI, Fig. S6 and S7†), revealed inductive and conjugative stabilisation of the carbene centres, in agreement with the generally accepted bonding scheme for NHCs.⁴⁷ The IBOs corresponding to the C–N σ -bonds were polarised towards the nitrogen atoms, whereas the nitrogen lone electron pairs were delocalised into the vacant 2p(C) orbital. In the IPr ligands, these two bonding components were symmetrical, but in the triazolylidene, the lone electron pair of the ferrocenyl-bound nitrogen atom contributed less than the nitrogen from the N–N bond. Thus, the better π -acceptor properties of the triazole ligand potentially resulted from the lower charge accumulated on the carbene carbon atom by conjugation ($\sum(\pi) = 0.83$ in the triazolylidene *vs.* $\sum(\pi) = 0.87$ in the IPr ligand). The lower π electron density at the carbene carbon in the triazolylidene thus reflected the replacement of one carbon in the conjugated double bond at the exterior for the more electronegative nitrogen, which reduced

Table 1 Selected experimental and calculated bond distances and the corresponding Mayer bond orders (MBO) and Wiberg bond indices (WBI)^a

Bond	Distance [Å]		MBO	WBI
	Exp.	Calc.		
Rh–C11	2.016(2)	2.007	0.69	1.04
Rh–I	2.6849(4)	2.721	0.82	1.54
Rh–C21	2.118(2)	2.101	0.66	0.84
Rh–C22	2.124(2)	2.124	0.68	0.80
Rh–C25	2.209(2)	2.209	0.59	0.66
Rh–C26	2.220(2)	2.220	0.54	0.63
C21–C22	1.410(3)	1.410	1.23	1.50
C25–C26	1.373(3)	1.373	1.42	1.64

^aTheoretical values were estimated at the PBE0(d3)/def2-TZVP:sdd(Rh, I) level of theory.

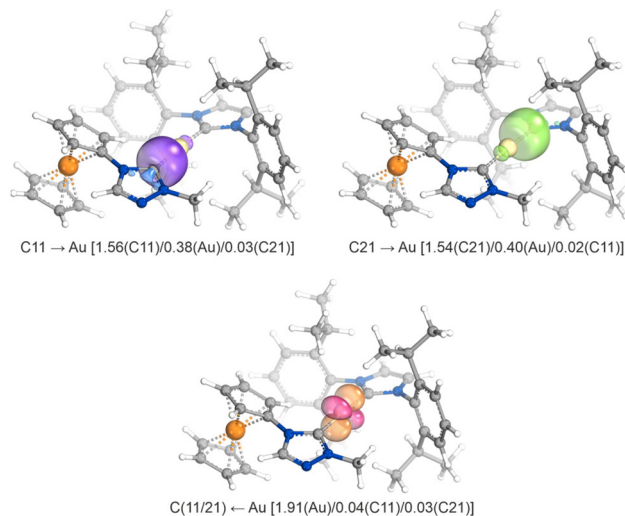


Fig. 7 Selected intrinsic bond orbitals (IBOs) of **4**. The values in parentheses indicate the fraction of bonding electrons assigned to the individual atoms. Atom labelling follows that in the crystal structure (see Fig. 2).

the net charge transferred to the carbene 2p(C) orbital from the adjacent nitrogen atoms.

Correspondingly, the IBO analysis of the hypothetical species [Au(SIPr){C(NMe)NCHN(Fc)}]⁺ (Fc = ferrocenyl) featuring the analogous, ring-saturated carbene ligand (SIPr = 1,3-bis(2,6-diisopropylphenyl)imidazolidin-2-ylidene) that lacks carbene stabilisation by the π electron density of the C=C or C=N bond showed that SIPr was indeed more electrophilic than the triazolylidene ligand. The cumulative charge contributed by the carbene π -system, $\sum(\pi)$, was 0.71. The overall back-donation from Au to the carbene carbons remained the same as that in **4** but was reversed in favour of the SIPr ligand [1.90(Au)/0.03(C^{triaz})/0.04(C^{SIPr})].

Conclusion

In this study, we describe the synthesis of 1,2,4-triazol-5-ylidene complexes bearing a redox-active ferrocenyl substituent directly at the heterocyclic carbene ligand from the readily accessible 4-ferrocenyl-4*H*-1,2,4-triazole. The reactions between the *N*-alkylated triazole and metal hydroxide/alkoxide precursors proceed cleanly, rapidly, and with a high atom economy, producing the targeted carbene complexes in good yields. The collected characterisation data, supported by the DFT calculations, corroborate the high *trans* influence of the triazolylidene ligand and the mode of stabilisation of the carbene moiety typical for NHCs based on the synergy between the inductive effect of the electronegative nitrogen atoms in the adjacent positions that reduces the σ electron density at the carbon atom and the conjugation between the nitrogen lone pairs and the carbene 2p orbital. Compared to IPr as a prototypical carbene ligand, the triazolylidene appears to be a slightly weaker σ donor and stronger π acceptor.



Experimental

Materials and methods

All syntheses were performed under a nitrogen atmosphere using standard Schlenk techniques and oven-dried glassware. Aminoferrocene⁴⁸ and $[(\text{IPr})\text{Au}(\text{OH})]$ ⁴⁹ were prepared by following the literature methods; the synthesis of **1** and **2** is described in the ESI.† Other chemicals were purchased from commercial suppliers (Sigma-Aldrich, TCI) and used as received. Toluene was dried over sodium metal and distilled under nitrogen. Dry dichloromethane was obtained from a PureSolv MD5 solvent purification system (Innovative Technology). Solvents used for chromatography and crystallisations were employed without any purification (Lach-Ner, analytical grade).

The NMR spectra were recorded on a Varian UNITY Inova 400 spectrometer at 25 °C. Chemical shifts (δ /ppm) are expressed relative to internal SiMe_4 . FTIR spectra were recorded with a Nicolet iS50 instrument (Thermo Fisher Scientific) over the 400–4000 cm^{-1} range. ESI MS spectra were recorded with a Compact QTOF-MS spectrometer (Bruker Daltonics). The samples were dissolved in HPLC-grade methanol. Elemental analyses were performed with a PE 2400 Series II CHNS/O Elemental Analyser (PerkinElmer). The amount of residual solvent was corroborated by NMR analysis.

Electrochemical measurements were carried out at room temperature using an μ AUTOLAB III instrument (Eco Chemie) and a three-electrode cell equipped with a glassy carbon disc (2 mm diameter) working electrode, a platinum auxiliary electrode, and an Ag/AgCl (3 M KCl) reference electrode. The samples were dissolved in dry dichloromethane to produce a solution containing approximately 1 mM of the analysed compound and 0.1 M $[\text{Bu}_4\text{N}][\text{PF}_6]$ as the supporting electrolyte (Sigma-Aldrich, puriss. for electrochemistry). The solutions were deaerated by bubbling with argon before the measurement and then maintained under an argon flow. Decamethylferrocene (Alfa-Aesar) was used as an internal standard during the last scans, and the potentials were converted into the ferrocene/ferrocenium scale by subtracting 0.548 V.⁵⁰

Details on the structure determination and DFT calculations are available in the ESI.†

Syntheses

Synthesis of 3. Solid $[\text{Rh}(\text{cod})(\mu\text{-OMe})]_2$ (24.2 mg, 0.050 mmol) was added to a solution of triazolium salt **2** (39.1 mg, 0.10 mmol) in dry dichloromethane (10 mL), and the resulting mixture was stirred at room temperature in the dark for 5 h and then concentrated under reduced pressure. The yellow-orange solid residue was purified by chromatography over silica gel and eluted with dichloromethane–methanol (75 : 1). The first yellow band was collected and evaporated, leaving complex **3** as a yellow-orange solid. Yield: 28.9 mg (73%). The single-crystal used for the structural determination was grown by dissolving the compound in acetone in a small vial and slowly diffusing water vapour in a large test tube.

¹H NMR (400 MHz, CDCl_3): δ 1.50–1.65 (m, 1H, CH_2 of cod), 1.67–1.79 (m, 1H, CH_2 of cod), 1.82–1.99 (m, 3H, CH_2 of cod), 2.12–2.39 (m, 3H, CH_2 of cod), 2.98–3.08 (m, 1H, CH of cod), 3.32–3.46 (m, 1H, CH of cod), 4.20 (s, 3H, CH_3), 4.24 (td, J = 2.6, 1.4 Hz, 1H, C_5H_4), 4.28 (s, 5H, C_5H_5), 4.35 (td, J = 2.6, 1.4 Hz, 1H, C_5H_4), 4.44 (td, J = 2.6, 1.4 Hz, 1H, C_5H_4), 5.25–5.33 (m, 2H, CH of cod), 6.36 (td, J = 2.6, 1.4 Hz, 1H, C_5H_4), 8.27 (s, 1H, NCH). ¹³C{¹H} NMR (151 MHz, CDCl_3): δ 29.52 (s, CH_2 of cod), 29.57 (s, CH_2 of cod), 31.57 (s, CH_2 of cod), 32.40 (s, CH_2 of cod), 40.74 (s, CH_3), 62.03 (s, CH of C_5H_4), 66.16 (s, CH of C_5H_4), 66.52 (s, CH of C_5H_4), 67.62 (s, CH of C_5H_4), 70.04 (s, C_5H_5), 71.90 (d, $^1J_{\text{C}-\text{Rh}}$ = 14 Hz, CH of cod), 72.53 (d, $^1J_{\text{C}-\text{Rh}}$ = 14 Hz, CH of cod), 92.95 (s, C^{ipso} –N of C_5H_4), 96.32 (d, $^1J_{\text{C}-\text{Rh}}$ = 7 Hz, CH of cod), 96.90 (d, $^1J_{\text{C}-\text{Rh}}$ = 7 Hz, CH of cod), 142.27 (s, NCH), 185.94 (d, $^1J_{\text{C}-\text{Rh}}$ = 49 Hz, C^{ipso} –Rh). ESI+ MS: m/z 478 ($[\text{M} - \text{I}]^+$). IR (DRIFTS, KBr): ν_{max} 3921 w, 3110 s, 3096 m, 3075 m, 3055 w, 2998 w, 2982 s, 2966 m, 2939 s, 2910 m, 2874 s, 2828 m, 1793 w, 1732 w, 1618 w, 1533 s, 1517 m, 1492 s, 1474 m, 1460 m, 1426 s, 1409 m, 1367 m, 1350 m, 1335 m, 1304 s, 1252 w, 1227 m, 1216 w, 1198 m, 1174 w, 1153 w, 1130 m, 1105 m, 1075 m, 1062 w, 1047 m, 1030 m, 1000 s, 993 m, 963 s, 959 s, 888 m, 877 s, 859 m, 843 m, 829 s, 824 s, 794 w, 784 m, 763 w, 720 m, 700 m, 681 w, 649 m, 637 w, 523 m, 506 s, 491 m, 471 s, 442 w, 430 w cm^{-1} . Anal. calc. for $\text{C}_{21}\text{H}_{25}\text{FeIN}_3\text{Rh}$ (605.10): C 41.68, H 4.16, N 6.94%. Found: C 41.94, H 4.08, N 6.91%.

Synthesis of 4. Gold(I) hydroxide $[(\text{IPr})\text{Au}(\text{OH})]$ (62.1 mg 0.10 mmol) was added to a solution of triazolium salt **2** (39.1 mg, 0.10 mmol) in dry dichloromethane (10 mL). The reaction mixture was stirred at ambient temperature in the dark for 5 h and then evaporated under reduced pressure. The solid residue was purified by chromatography over a short silica gel column using dichloromethane–methanol (20 : 1). Evaporation of a single yellow band produced complex **4** as a yellow-orange solid. The yield of **4**· $2\text{CH}_2\text{Cl}_2$ was 92.0 mg (90%). The crystal used for structure determination was obtained from a dichloromethane solution layered with methyl *tert*-butyl ether.

¹H NMR (400 MHz, CDCl_3): δ 1.22 (d, $^3J_{\text{HH}}$ = 6.9 Hz, 12H, CHMe_2), 1.27 (d, $^3J_{\text{HH}}$ = 6.9 Hz, 12H, CHMe_2), 2.52 (sept, $^3J_{\text{HH}}$ = 6.9 Hz, 4H, CHMe_2), 3.28 (s, 3H, CH_3), 3.96 (t, J = 2.0 Hz, 2H, C_5H_4), 4.16 (s, 5H, C_5H_5), 4.40 (t, J = 2.0 Hz, 2H, C_5H_4), 7.36 (d, J = 7.8 Hz, 4H, Ph), 7.52 (s, 2H, $\text{CH}=\text{CH}$ of IPr), 7.61 (t, J = 7.8 Hz, 2H, Ph), 8.99 (s, 1H, NCH of triazole). ¹³C{¹H} NMR (150 MHz, CDCl_3): δ 24.03 (s, CHMe_2), 24.85 (s, CHMe_2), 28.87 (s, CHMe_2), 39.36 (s, CH_3), 63.56 (s, CH of C_5H_4), 67.14 (s, CH of C_5H_4), 70.24 (s, C_5H_5), 91.49 (s, C^{ipso} –N of C_5H_4), 124.38 (s, CH of Ph), 124.78 (s, $\text{CH}=\text{CH}$ of IPr), 131.05 (s, CH of Ph), 133.59 (s, C^{ipso} –N of Ph), 144.06 (s, NCH of triazole), 145.88 (s, C^{ipso} – CHMe_2 of IPr), 183.46 (s, C^{ipso} –Au of triazolylidene), 185.46 (s, C^{ipso} –Au of IPr). ESI+ MS: m/z 852 ($[\text{M} - \text{I}]^+$). IR (DRIFTS, KBr): ν_{max} 3568 w, 3357 w, 3110 m, 3071 m, 3024 m, 2960 s, 2926 s, 2868 m, 2711 w, 1725 w, 1621 w, 1592 w, 1533 m, 1492 s, 1471 s, 1459 s, 1423 m, 1400 w, 1386 m, 1364 m, 1351 m, 1329 m, 1311 m, 1274 s, 1250 s, 1241 s, 1220 s, 1182 m, 1146 m, 1126 w, 1107 m, 1061 m, 1017 s, 978 m,



949 w, 938 w, 874 m, 820 s, 811 s, 804 s, 759 s, 727 s, 719 s, 712 m, 674 w, 655 m, 640 w, 608 m, 576 m, 549 w, 534 w, 493 s, 474 m, 452 m, 431 w cm^{-1} . Anal. calc. for $\text{C}_{40}\text{H}_{49}\text{AuFeIN}_5 \cdot 1/2\text{CH}_2\text{Cl}_2$ (1022.03): C 47.59, H 4.93, N 6.85%. Found: C 47.52, H 4.88, N 6.87%.

Data availability

The data will be available upon reasonable request.

Conflicts of interest

There are no conflicts to declare.

Acknowledgements

This work was supported by the Czech Science Foundation (project no. 23-06718S). Theoretical calculations were performed using the resources provided by the e-INFRA CZ project (ID: 90254), supported by the Ministry of Education, Youth and Sports of the Czech Republic. The authors also thank Dr Ivana Císařová from the Department of Inorganic Chemistry, Faculty of Science, Charles University, for collecting the X-ray diffraction data.

Notes and references

- (a) H.-W. Wanzlick and E. Schikora, *Angew. Chem.*, 1960, **72**, 49; (b) H.-W. Wanzlick and E. Schikora, *Chem. Ber.*, 1961, **64**, 2389; (c) H.-W. Wanzlick, *Angew. Chem., Int. Ed. Engl.*, 1962, **1**, 75.
- (a) K. Öfele, *J. Organomet. Chem.*, 1968, **12**, P42 See also: (b) D. J. Cardin, B. Cetinkaya and M. F. Lappert, *Chem. Rev.*, 1972, **72**, 545; (c) M. F. Lappert, *J. Organomet. Chem.*, 1988, **358**, 185.
- The very first isolable carbene, $\text{R}_2\text{PCSiMe}_3$, was reported even earlier in: A. Igau, H. Grützmacher, A. Baceiredo and G. Bertrand, *J. Am. Chem. Soc.*, 1988, **110**, 6463.
- (a) A. J. Arduengo, R. L. Harlow and M. Kline, *J. Am. Chem. Soc.*, 1991, **113**, 361; (b) A. J. Arduengo, H. V. R. Dias, R. L. Harlow and M. Kline, *J. Am. Chem. Soc.*, 1992, **114**, 5530; (c) A. J. Arduengo, J. R. Goerlich and W. J. Marshall, *J. Am. Chem. Soc.*, 1995, **117**, 11027.
- (a) F. E. Hahn and M. C. Jahnke, *Angew. Chem., Int. Ed.*, 2008, **47**, 3122; (b) P. de Frémont, N. Marion and S. P. Nolan, *Coord. Chem. Rev.*, 2009, **293**, 862; (c) D. J. Nelson and S. P. Nolan, *Chem. Soc. Rev.*, 2013, **42**, 6723; (d) M. N. Hopkinson, C. Richter, M. Schedler and F. Glorius, *Nature*, 2014, **510**, 485; (e) H. V. Huynh, *Chem. Rev.*, 2018, **118**, 9457; (f) P. Bellotti, M. Koy, M. N. Hopkinson and F. Glorius, *Nat. Rev. Chem.*, 2021, **5**, 711.
- 1,2,3-Triazoles are accessible by Cu-catalysed Huisgen cycloaddition from azides and alkynes: (a) M. Meldal and C. Wenzel Tornøe, *Chem. Rev.*, 2008, **108**, 2952; (b) M. Breugst and H.-U. Reissig, *Angew. Chem., Int. Ed.*, 2020, **59**, 12293.
- (a) P. Mathew, A. Neels and M. Albrecht, *J. Am. Chem. Soc.*, 2008, **130**, 13534 For reviews, see: (b) O. Schuster, L. Yang, H. G. Raubenheimer and M. Albrecht, *Chem. Rev.*, 2009, **109**, 3445; (c) R. H. Crabtree, *Coord. Chem. Rev.*, 2013, **257**, 755; (d) G. Guisado-Barrios, M. Soleilhavoup and G. Bertrand, *Acc. Chem. Res.*, 2018, **51**, 3236; (e) Á. Vivancos, C. Segarra and M. Albrecht, *Chem. Rev.*, 2018, **118**, 9493; (f) R. Maity and B. Sarkar, *JACS Au*, 2022, **2**, 22.
- D. Enders, K. Breuer, G. Raabe, J. Runsink, J. H. Teles, J.-P. Melder, K. Ebel and S. Brode, *Angew. Chem., Int. Ed. Engl.*, 1995, **34**, 1021.
- 1,2,4-Triazole-5-ylidenes remained overlooked; the carbene character of the long known analytical reagent nitron has been recognized only relatively recently: C. Färber, M. Leibold, C. Bruhn, M. Maurer and U. Siemeling, *Chem. Commun.*, 2012, **48**, 227.
- Representative examples: (a) F. Simal, D. Jan, L. Delaude, A. Demonceau, M.-R. Spirlet and A. F. Noels, *Can. J. Chem.*, 2001, **79**, 529; (b) A. Zanardi, R. Corberán, J. A. Mata and E. Peris, *Organometallics*, 2008, **27**, 3570; (c) J. Iglesias-Sigüenza, A. Ros, E. Díez, M. Alcarazo, E. Álvarez, R. Fernández and J. M. Lassaletta, *Dalton Trans.*, 2009, 7113; (d) C. Dash, M. M. Shaikh and P. Ghosh, *Eur. J. Inorg. Chem.*, 2009, 1608; (e) S. K. U. Riederer, P. Gigler, M. P. Högerl, E. Herdtweck, B. Bechlars, W. A. Herrmann and F. E. Kühn, *Organometallics*, 2010, **29**, 5681; (f) C. Dash, M. M. Shaikh, R. J. Butcher and P. Ghosh, *Dalton Trans.*, 2010, **39**, 2515; (g) S. K. U. Riederer, B. Bechlars, W. A. Herrmann and F. E. Kühn, *Dalton Trans.*, 2011, **40**, 41; (h) S. C. Holm, F. Rominger and B. F. Straub, *J. Organomet. Chem.*, 2012, **719**, 54; (i) J. Turek, I. Panov, M. Semler, P. Štěpnička, F. De Proft, Z. Padělková and A. Růžička, *Organometallics*, 2014, **33**, 3108; (j) D. Yuan and H. V. Huynh, *Organometallics*, 2014, **33**, 6033; (k) S. K. Gupta, S. K. Sahoo and J. Choudhury, *Organometallics*, 2016, **35**, 2462; (l) V. H. Nguyen, M. B. Ibrahim, W. W. Mansour, B. M. El Ali and H. V. Huynh, *Organometallics*, 2017, **36**, 2345; (m) V. H. Nguyen, B. M. El Ali and H. V. Huynh, *Organometallics*, 2018, **37**, 2358; (n) V. H. Nguyen, H. H. Nguyen and H. H. Do, *Inorg. Chem. Commun.*, 2020, **121**, 108173; (o) M. T. Lee, M. B. Goodstein and G. Lalic, *J. Am. Chem. Soc.*, 2019, **141**, 17086; (p) V. H. Nguyen, T. T. Dang, H. H. Nguyen and H. V. Huynh, *Organometallics*, 2020, **39**, 2309; (q) S. Bauri, A. Mallik and A. Rit, *Organometallics*, 2020, **39**, 3362; (r) P. J. Quinlivan, A. Loo, D. G. Shlian, J. Martinez and G. Parkin, *Organometallics*, 2021, **40**, 166; (s) H.-Y. Hung, Y.-H. Hsu, H.-C. Pi, C.-H. Hu and H. M. Lee, *Dalton Trans.*, 2022, **51**, 18264.



11 (a) K. M. Lee, H. M. J. Wang and I. J. B. Lin, *J. Chem. Soc., Dalton Trans.*, 2002, 2852; (b) Y. Unger, D. Meyer and T. Strassner, *Dalton Trans.*, 2010, **39**, 4295; (c) M. Tenne, S. Metz, I. Muenster, G. Wagenblast and T. Strassner, *Organometallics*, 2013, **32**, 6257; (d) M. Tenne, S. Metz, G. Wagenblast, I. Muenster and T. Strassner, *Dalton Trans.*, 2015, **44**, 8444; (e) S. Aghazada, I. Zimmermann, V. Scutelnic and M. K. Nazeeruddin, *Organometallics*, 2017, **36**, 2397; (f) J. Soellner and T. Strassner, *Organometallics*, 2018, **37**, 1821; (g) B.-S. Yun, S.-Y. Kim, J.-H. Kim, S. Choi, S. Lee, H.-J. Son and S. O. Kang, *ACS Appl. Electron. Mater.*, 2022, **4**, 2699.

12 (a) A. Kumar, A. Naaz, A. P. Prakasham, M. K. Gangwar, R. J. Butcher, D. Panda and P. Ghosh, *ACS Omega*, 2017, **2**, 4632; (b) Y. Gothe, I. Romero-Canelón, T. Marzo, P. J. Sadler, L. Messori and N. Metzler-Nolte, *Eur. J. Inorg. Chem.*, 2018, 2461; (c) J. C. Mather, J. A. Wyllie, A. Hamilton, T. P. Soares da Costa and P. J. Barnard, *Dalton Trans.*, 2022, **51**, 12056; (d) H. T. T. Phung, H.-M. Vu, M. Q. H. Ly, H. H. Nguyen, T. H. Nguyen, H. T. T. Luong and V. H. Nguyen, *Inorg. Chem. Commun.*, 2023, **154**, 110898.

13 (a) D. Enders, O. Niemeier and A. Henseler, *Chem. Rev.*, 2007, **107**, 5606; (b) D. M. Flanigan, F. Romanov-Michaillidis, N. A. White and T. Rovis, *Chem. Rev.*, 2015, **115**, 9307.

14 (a) U. Siemeling, *Eur. J. Inorg. Chem.*, 2012, 3523; (b) P. Štěpnička, *Dalton Trans.*, 2022, **51**, 8085.

15 (a) L. Hettmanczyk, S. Manck, C. Hoyer, S. Hohloch and B. Sarkar, *Chem. Commun.*, 2015, **51**, 10949; (b) L. Hettmanczyk, L. Suntrup, S. Klenk, C. Hoyer and B. Sarkar, *Chem. – Eur. J.*, 2017, **23**, 576; (c) D. Aucamp, T. Witteler, F. Dielmann, S. Siangwata, D. C. Liles, G. S. Smith and D. I. Bezuidenhout, *Eur. J. Inorg. Chem.*, 2017, 1227; (d) S. Klenk, S. Rupf, L. Suntrup, M. van der Meer and B. Sarkar, *Organometallics*, 2017, **36**, 2026; (e) D. Aucamp, S. V. Kumar, D. C. Liles, M. A. Fernandes, L. Harmse and D. I. Bezuidenhout, *Dalton Trans.*, 2018, **47**, 16072; (f) R. Haraguchi, S. Hoshino, T. Yamazaki and S. Fukuzawa, *Chem. Commun.*, 2018, **54**, 2110; (g) R. Haraguchi, T. Yamazaki, K. Torita, T. Ito and S. Fukuzawa, *Dalton Trans.*, 2020, **49**, 17578; (h) K. Škoch, P. Vosáhlo, I. Císařová and P. Štěpnička, *Dalton Trans.*, 2020, **49**, 1011; (i) C. Hoyer, P. Schwerk, L. Suntrup, J. Beerhues, M. Nössler, U. Albold, J. Dernedde, K. Tedin and B. Sarkar, *Eur. J. Inorg. Chem.*, 2021, 1373.

16 G. Forcher, A. Silvanus, P. de Frémont, B. Jacques, M. S. M. Pearson-Long, F. Boeda and P. Bertus, *J. Organomet. Chem.*, 2015, **797**, 1.

17 Some 1,2,4-triazoles with ferrocenyl substituents have been studied as N-donor ligands. For examples, see: (a) G. Gasser, J. D. Carr, S. J. Coles, S. J. Green, M. B. Hursthouse, S. M. Cafferkey, H. Stoeckli-Evans and J. H. R. Tucker, *J. Organomet. Chem.*, 2010, **695**, 249; (b) H. S. Scott, A. Nafady, J. D. Cashion, A. M. Bond, B. Moubaraki, K. S. Murray and S. M. Neville, *Dalton Trans.*, 2013, **42**, 10326.

18 T. Mochida, H. Shimizu, S. Suzuki and T. Akasaka, *J. Organomet. Chem.*, 2006, **691**, 4882.

19 (a) H. E. Bryndza and W. Tam, *Chem. Rev.*, 1988, **88**, 1163; (b) D. J. Nelson and S. P. Nolan, *Coord. Chem. Rev.*, 2017, **353**, 278.

20 S. Sethi, P. Kumar Das and N. Behera, *J. Organomet. Chem.*, 2016, **824**, 140.

21 R. K. Bartlett and I. R. Humphrey, *J. Chem. Soc. C*, 1967, 1664.

22 The yield significantly decreased when undried solvent or noninert conditions were used.

23 Y. Miura, F. Shimizu and T. Mochida, *Inorg. Chem.*, 2010, **49**, 10032.

24 T. J. Curphey and K. D. Prasad, *J. Org. Chem.*, 1972, **37**, 2259.

25 (a) A. Zanardi, J. A. Mata and E. Peris, *J. Am. Chem. Soc.*, 2009, **131**, 14531; (b) A. Zanardi, J. A. Mata and E. Peris, *Organometallics*, 2009, **28**, 4335; (c) A. Zanardi, J. A. Mata and E. Peris, *Chem. – Eur. J.*, 2010, **16**, 13109; (d) S. Sabater, J. A. Mata and E. Peris, *Chem. – Eur. J.*, 2012, **18**, 6380; (e) S. Guo and H. V. Huynh, *Organometallics*, 2012, **31**, 4565; (f) S. Guo and H. V. Huynh, *Organometallics*, 2014, **33**, 2004, and ref. 10b.

26 Recently, Hölzel and Ganter achieved two-fold methylation of a 1,2,4-triazole upon reacting 5-(dimethylamino)-1,4-dimethyl-4*H*-1,2,4-triazol-1-ium iodide with an excess of methyl triflate: T. Hölzel and C. Ganter, *J. Organomet. Chem.*, 2020, **915**, 121234.

27 D. C. D. Butler and C. J. Richards, *Organometallics*, 2002, **21**, 5433.

28 (a) C. Köcher and W. A. Herrmann, *J. Organomet. Chem.*, 1997, **532**, 261; (b) M. V. Baker, S. K. Brayshaw, B. W. Skelton and A. H. White, *Inorg. Chim. Acta*, 2004, **357**, 2841.

29 (a) S. P. Nolan, *Acc. Chem. Res.*, 2011, **44**, 91; (b) T. Scattolin, G. Tonon, E. Botter, S. G. Guillet, N. V. Tzouras and S. P. Nolan, *Chem. – Eur. J.*, 2023, **29**, e202301961.

30 For an analogous reaction with a triazolium salt, see: S. Gaillard, P. Nun, A. M. Z. Slawin and S. P. Nolan, *Organometallics*, 2010, **29**, 5402.

31 (a) T. G. Appleton, H. C. Clark and L. E. Manzer, *Coord. Chem. Rev.*, 1973, **10**, 335; (b) F. R. Hartley, *Chem. Soc. Rev.*, 1973, **2**, 163.

32 (a) S. Fuertes, A. J. Chueca and V. Sicilia, *Inorg. Chem.*, 2015, **54**, 9885; (b) F. Horký, J. Soellner, J. Schulz, I. Císařová, T. Strassner and P. Štěpnička, *New J. Chem.*, 2023, **47**, 18442.

33 J. Iglesias-Sigüenza, A. Ros, E. Díez, M. Alcarazo, E. Álvarez, R. Fernández and J. M. Lassaletta, *Dalton Trans.*, 2009, 7113.

34 T. Hölzel, M. Otto, H. Buhl and C. Ganter, *Organometallics*, 2017, **36**, 4443.

35 J. C. Green, *Chem. Soc. Rev.*, 1998, **27**, 263.



36 S. Gaillard, J. Bosson, R. S. Ramón, P. Nun, A. M. Z. Slawin and S. P. Nolan, *Chem. – Eur. J.*, 2010, **16**, 13729.

37 Q. Liu, M. Xie, X. Chang, S. Cao, C. Zou, W.-F. Fu, C.-M. Che, Y. Chen and W. Lu, *Angew. Chem., Int. Ed.*, 2018, **57**, 6279.

38 G. Gritzner and J. Kúta, *Pure Appl. Chem.*, 1984, **56**, 461.

39 S. Wolf and H. Plenio, *J. Organomet. Chem.*, 2009, **694**, 1487.

40 T. Lu and F. Chen, *Acta Chim. Sin.*, 2011, **69**, 2393.

41 (a) J. Schulz, F. Uhlík, J. M. Speck, I. Císařová, H. Lang and P. Štěpnička, *Organometallics*, 2014, **33**, 5020; (b) K. Škoch, I. Císařová, F. Uhlík and P. Štěpnička, *Dalton Trans.*, 2018, **47**, 16082; (c) K. Škoch, J. Schulz, I. Císařová and P. Štěpnička, *Organometallics*, 2019, **38**, 3060; (d) P. Vosáhlo, J. Schulz, I. Císařová and P. Štěpnička, *Dalton Trans.*, 2021, **50**, 6232.

42 (a) G. Knizia, *J. Chem. Theory Comput.*, 2013, **9**, 4834; (b) G. Knizia and J. E. M. N. Klein, *Angew. Chem., Int. Ed.*, 2015, **54**, 5518. For applications in the chemistry of carbene ligands, see: (c) L. Nunes dos Santos Comprido, J. E. M. N. Klein, G. Knizia, J. Kästner and A. S. K. Hashmi, *Angew. Chem., Int. Ed.*, 2015, **54**, 10336; (d) F. F. Mulks, A. S. K. Hashmi and S. Faraji, *Organometallics*, 2020, **39**, 1814; (e) L. Nunes dos Santos Comprido, J. E. M. N. Klein, G. Knizia, J. Kästner and A. S. K. Hashmi, *Chem. – Eur. J.*, 2016, **22**, 2892; (f) D. Sorbelli, L. Nunes dos Santos Comprido, G. Knizia, A. S. K. Hashmi, L. Belpassi, P. Belanzoni and J. E. M. N. Klein, *ChemPhysChem*, 2019, **20**, 1671.

43 (a) M. J. S. Dewar, *Bull. Soc. Chim. Fr.*, 1951, **18**, C71; (b) J. Chatt and L. A. Duncanson, *J. Chem. Soc.*, 1953, 2939.

44 (a) R. G. Pearson, *Inorg. Chem.*, 1973, **12**, 712, and ref. 32.

45 M. L. H. Green, *J. Organomet. Chem.*, 1995, **500**, 127.

46 (a) X. Hu, I. Castro-Rodriguez, K. Olsen and K. Meyer, *Organometallics*, 2004, **23**, 755; (b) D. M. Khramov, V. M. Lynch and C. W. Bielawski, *Organometallics*, 2007, **26**, 6042; (c) D. Nemesok, K. Wichmann and G. Frenking, *Organometallics*, 2004, **23**, 3640; (d) S. V. C. Vummaleti, D. J. Nelson, A. Poater, A. Gómez-Suárez, D. B. Cordes, A. M. Z. Slawin, S. P. Nolan and L. Cavallo, *Chem. Sci.*, 2015, **6**, 1895; (e) G. Bistoni, L. Belpassi and F. Tarantelli, *Angew. Chem., Int. Ed.*, 2013, **52**, 11599.

47 (a) C. Heinemann, T. Müller, Y. Apeloig and H. Schwarz, *J. Am. Chem. Soc.*, 1996, **118**, 2023; (b) W. A. Herrmann and C. Köcher, *Angew. Chem., Int. Ed. Engl.*, 1997, **36**, 2162; (c) D. Bourissou, O. Guerret, F. P. Gabbai and G. Bertrand, *Chem. Rev.*, 2000, **100**, 39.

48 A. Leonidova, T. Joshi, D. Nipkow, A. Frei, J.-E. Penner, S. Konatschnig, M. Patra and G. Gasser, *Organometallics*, 2013, **32**, 2037.

49 S. Gaillard, A. M. Z. Slawin and S. P. Nolan, *Chem. Commun.*, 2010, **46**, 2742.

50 F. Barrière and W. E. Geiger, *J. Am. Chem. Soc.*, 2006, **128**, 3980.

